

# Spin-wave dispersion in orbitally ordered $\text{La}_{1/2}\text{Sr}_{3/2}\text{MnO}_4$

D. Senff,<sup>1</sup> F. Krüger,<sup>2,3</sup> S. Scheidl,<sup>2</sup> M. Benomar,<sup>1</sup> Y. Sidis,<sup>4</sup> F. Demmel,<sup>5</sup> and M. Braden<sup>1,\*</sup>

<sup>1</sup>*II. Physikalisches Institut, Universität zu Köln, Zùlpicher Str. 77, D-50937 Köln, Germany*

<sup>2</sup>*Institut für Theoretische Physik, Universität zu Köln, Zùlpicher Str. 77, D-50937 Köln, Germany*

<sup>3</sup>*Instituut-Lorentz, Universiteit Leiden, P.O. Box 9506, 2300 RA Leiden, The Netherlands*

<sup>4</sup>*Laboratoire Léon Brillouin, C.E.A./C.N.R.S., F-91191 Gif-sur-Yvette Cedex, France*

<sup>5</sup>*Institut Laue-Langevin, Boîte Postale 156, 38042 Grenoble Cedex 9, France*

(Dated: November 6, 2018, **preprint**)

The magnon dispersion in the charge, orbital and spin ordered phase in  $\text{La}_{1/2}\text{Sr}_{3/2}\text{MnO}_4$  has been studied by means of inelastic neutron scattering. We find an excellent agreement with a magnetic interaction model basing on the CE-type superstructure. The magnetic excitations are dominated by ferromagnetic exchange parameters revealing a nearly-one dimensional character at high energies. The nearest neighbor ferromagnetic interaction in  $\text{La}_{1/2}\text{Sr}_{3/2}\text{MnO}_4$  is significantly larger than the one in the metallic ferromagnetically ordered manganites. The large ferromagnetic interaction in the charge/orbital ordered phase appears to be essential for the capability of manganites to switch between metallic and insulating phases.

PACS numbers: 75.20.-m, 71.10.-w, 75.47.Lx, 75.50.Ee, 75.25.+z

The phenomenon of colossal magneto-resistivity in the manganites is only partially explained by the Zener double-exchange mechanism, the larger part of it appears to arise from the competition of two states : the metallic ferromagnetically ordered state on the one side and the insulating one with a cooperative ordering of charges, orbitals and spins (COS) on the other side [1, 2]. The insulator to metal transition consists in switching from a phase with long or short-range COS-correlations into the metallic state where spins are aligned either by external field or by spontaneous magnetic order. Such interpretation is strongly supported by studies of the diffuse scattering related with the COS-correlations: the decrease in electronic resistivity is found to scale with the suppression of diffuse scattering as function of either temperature [3, 4] or of magnetic field [5].

In spite of its eminent relevance for colossal magneto-resistivity the exact nature of the COS-states in the manganites has not yet been fully established. The combined COS-ordering has first been studied in the pioneer work by Wollan and Koehler [6] and by Goodenough [7] proposing the so-called CE-type arrangement, which is illustrated in Fig. 1a). For half doping, i.e. equal amounts of the  $\text{Mn}^{3+}$  and  $\text{Mn}^{4+}$ , there is a checkerboard arrangement of different charges. In addition the  $e_g$ -orbitals at the  $\text{Mn}^{3+}$  sites form zigzag-chains. The CE-type charge and orbital arrangement will yield a ferromagnetic interaction in the zigzag-chains and an antiferromagnetic one in-between. In the recent literature there is evidence both for [8, 9] and against [10] this CE-type picture of the COS-state near half doping. The quantitative structural analysis excludes a full ordering of charges and orbitals [8, 9] which would induce stronger structural distortions. Recently, a qualitatively different scheme was proposed for  $\text{Pr}_{0.6}\text{Ca}_{0.4}\text{MnO}_3$  where charges do not order on the metal sites but on the Mn-O-Mn bonds forming Zener

polarons [10]. Whether this Zener-polaron picture is applicable for all manganites or whether it is relevant at all is still under debate [11].

The magnetic excitations in the ferromagnetic metallic manganites have been studied by inelastic neutron scattering in many different compositions [12, 13, 14, 15], for a recent summary see reference [15]. At low  $\mathbf{q}$  the dispersion is qualitatively similar in all compounds, it is isotropic and quadratic,  $\omega = Dq^2$ , with spin stiffness constants of the order of  $D \sim 150$  meV. However at large  $\mathbf{q}$ , the spin-wave dispersion is depending on the exact composition and it is rather anisotropic. An anomalous softening of the magnons at the zone-boundaries has been recently attributed to extended exchange-coupling constants arising from orbital effects [15]. In view of the large amount of data on the ferromagnetic phases, it may astonish that there is still no detailed study on the magnetic excitations in the antiferromagnetic COS-states. Besides the intrinsic complexity of the CE-type magnetic ordering, such a study is severely hampered by the twinning of the manganite crystals in the perovskite phases. We, therefore, have chosen the layered material  $\text{La}_{1/2}\text{Sr}_{3/2}\text{MnO}_4$  to study the magnon dispersion in the COS-state. We obtain the full dispersion of the two magnon branches with lowest energies which may be satisfactorily described in the CE-type model.

The structural, electronic and magnetic phase diagram of  $\text{La}_{1+x}\text{Sr}_{1-x}\text{MnO}_4$  has been elaborated in references [16, 17, 18]. For  $x=0$ ,  $\text{LaSrMnO}_4$ , all Mn are three-valent with occupation of  $(3z^2 - r^2)$   $e_g$ -orbitals and spin order antiferromagnetically. The half-doped compound,  $\text{La}_{1/2}\text{Sr}_{3/2}\text{MnO}_4$ , exhibits the cooperative COS ordering, which has been studied by various techniques [19, 20, 21, 22, 23]. Compared to most perovskite manganites at half doping, the COS-state in  $\text{La}_{1/2}\text{Sr}_{3/2}\text{MnO}_4$  appears to be rather stable, only in very high magnetic fields of the

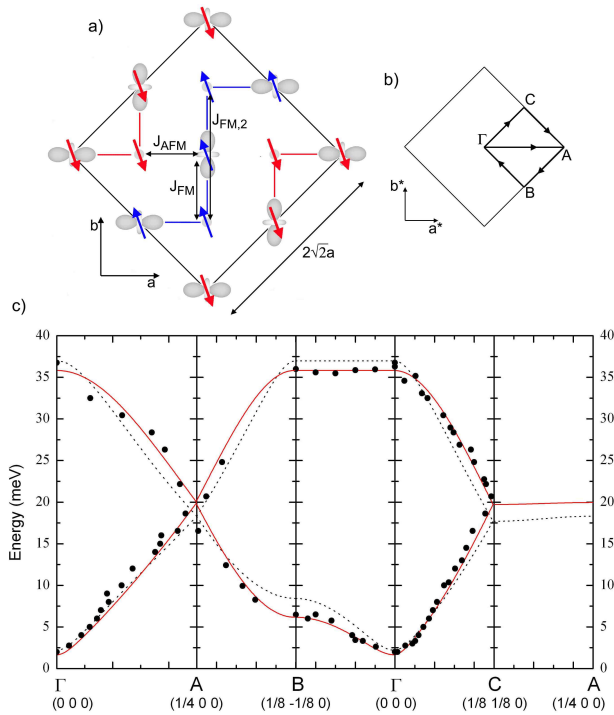


FIG. 1: (color online) a) Schematic representation of the CE-type ordering in the  $ab$ -plane of half doped manganites with the three magnetic interactions parameters described in the text. Notice, that the FM zigzag-chains run along the  $[110]$ -direction. b) Sketch of the magnetic Brillouin-zone, displaying the high symmetry points  $\Gamma = (0, 0, 0)$ ,  $A = (1/4, 0, 0)$ ,  $B = (1/8, -1/8, 0)$ ,  $C = (1/8, 1/8, 0)$  and the path of the calculated dispersion. c) Dispersion of the magnetic excitations in  $\text{La}_{1/2}\text{Sr}_{3/2}\text{MnO}_4$  in a direction parallel  $[100]$  ( $\Gamma$  to A), perpendicular to the chains ( $\Gamma$  to B) and parallel to the chains ( $\Gamma$  to C). The solid and broken lines give the spin-wave dispersion calculated with two parameter sets, see text.

order of 30 T the COS-state is suppressed and colossal magnetoresistivity is observed [24]. For the study of the magnetic excitations in the COS-state this material is nevertheless well suited.

The single crystal used in this study was grown by the floating zone technique as described in [25] (volume  $0.6\text{cm}^3$ , space group  $I4/mmm$ ,  $a=3.86\text{\AA}$  and  $c=12.42\text{\AA}$  at room temperature). Upon cooling we observe the sequence of structural and magnetic ordering following the appearance of the respective superstructure reflections in neutron diffraction experiments. Orbital and charge ordering within the CE-type picture is related with superstructure reflections displaced from reciprocal lattice vectors by  $\mathbf{q}=(\pm\frac{1}{4}, \pm\frac{1}{4}, 0)$  and by  $(\pm\frac{1}{2}, \pm\frac{1}{2}, 0)$  respectively (we use reduced lattice units of  $\frac{2\pi}{a}$  with respect to the  $I4/mmm$  cell). The onset of charge/orbital ordering is observed at  $T_{CO/OO} = 230\text{K}$  in agreement with references [19, 21]. In addition, below  $T_N = 110\text{K}$  antiferromagnetic ordering is evidenced through magnetic reflections [19]; the magnetic ordering remains, however, to a

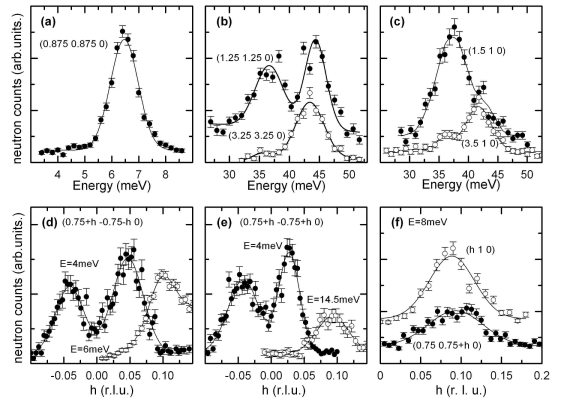


FIG. 2: (color online) Raw-data scans to determine the magnon dispersion in  $\text{La}_{1/2}\text{Sr}_{3/2}\text{MnO}_4$ , symbols denote data and lines fits with gaussians. a-c) Constant  $\mathbf{Q}$  scans at antiferromagnetic zone-center and zone-boundaries (b) and (c) were measured with  $E_f = 7.37\text{meV}$  and using the copper-monochromator); the different  $\mathbf{Q}$ -dependence separates magnetic from phononic scattering in b) and c). d-f) : Constant energy scans for different energies across  $(0.75, -0.75, 0)$  in  $[1, \bar{1}, 0]$ -direction, i.e. perpendicular to the zigzag-chains d), and in  $[1, 1, 0]$ -direction e), i.e. parallel to the zigzag-chains. f) Scan aiming at the dispersion along the  $[0, 1, 0]$ -direction, path  $\Gamma$ -A.

large extent two-dimensional in nature in our as well as in previously studied crystals [19]. For the determination of the magnon-dispersion the lack of correlations along the  $c$ -direction is irrelevant, as the magnetic exchange parameters are negligible along this direction. In the following, we only discuss the layered magnetic ordering.

Let us illustrate the different propagation vectors with the aid of the scheme given in Fig. 1a). With the orbital ordering, the nuclear lattice gets orthorhombic with lattice constants of  $\sqrt{2}a$  along  $[1, \bar{1}, 0]$  and  $2\sqrt{2}a$  along  $[1, 1, 0]$ . Note that the zigzag-chains run along the  $[1, 1, 0]$ -direction. Orbital ordering is only related to superstructure reflections with  $\mathbf{q}=\pm(\frac{1}{4}, \frac{1}{4}, 0)$ . Considering only the  $\text{Mn}^{3+}$ -sites the magnetic lattice is orthorhombic too and of the same size as the structural one but rotated by  $90^\circ$ ,  $2\sqrt{2}a$  along  $[1, \bar{1}, 0]$  and  $\sqrt{2}a$  along  $[1, 1, 0]$ . The  $\text{Mn}^{3+}$ -spins contribute to magnetic superstructure reflections with  $\mathbf{q}=\pm(\frac{1}{4}, -\frac{1}{4}, 0)$ , for example there is a contribution at  $(0.25, 0.75, 0)=(0.25, -0.25, 0)$  but none at  $(0.25, 0.25, 0)$ . The  $\text{Mn}^{4+}$ -spins do not contribute to neither of these but to positions with  $\mathbf{q}=\pm(0, 0.5, 0)$  or  $\mathbf{q}=\pm(0.5, 0, 0)$ , where the  $\text{Mn}^{3+}$ -spins do not contribute. The full magnetic cell has to be described in a pseudo-quadratic lattice with constants  $2\sqrt{2}a$  along  $[1, \bar{1}, 0]$  and  $[1, 1, 0]$ , as shown in Fig. 1a). Due to the twinning in the orthorhombic COS-phase the arrangement in Fig. 1a) (orientation I) is superposed by the same rotated by  $90^\circ$  (orientation II) in a sample crystal. Both twin orientations contribute equally in our sample, but we will always refer to orientation I for the analysis.

Neutron scattering experiments were performed on the triple-axis spectrometers *4F* and *1T* at the Orphée reactor in Saclay, France, and on *IN3* at the ILL in Grenoble, France. The sample was mounted with the [001]-direction perpendicular to the scattering plane and cooled to  $T=15$  K. Monochromatic neutrons were selected using Bragg-scattering from the (002)-reflection of pyrolytic graphite (PG) or – at higher incident energies – the (111)-reflection of copper. The final energies of the scattered neutrons were in most cases fixed to 14.7 meV, to suppress higher order contaminations with the aid of a PG-filter.

The magnon dispersion in  $\text{La}_{1/2}\text{Sr}_{3/2}\text{MnO}_4$  was determined by scanning with either  $\mathbf{Q}$  or the energy transfer kept constant. At the antiferromagnetic zone center we find a gap in the magnetic excitation spectrum and a small energy-splitting of the lowest excitation. The degeneracy of the two transverse magnons appears to be lifted due to complex magnetic anisotropy terms, see [26]. Already for  $q > 3.9 \cdot 10^{-3} \text{ \AA}^{-1}$  away from the zone-centre, no splitting in the magnon frequencies is resolved anymore. In spite of the twinning of the crystal in the COS-phase we are able to separate the magnon branches parallel and perpendicular to the zigzag-chains, as only one twin orientation contributes to a quarter-indexed magnetic superstructure reflection. When going from the antiferromagnetic zone center (0.75,-0.75,0) along the [1,1,0]-direction one determines the spin-wave dispersion parallel to the zigzag-chains (see Fig. 2e)) and when going along the  $[1, \bar{1}, 0]$ -direction one measures the dispersion perpendicular to the chains. This behavior is corroborated by the structure factor calculations presented in Fig. 3 as discussed below. The raw-data scans shown in Fig. 2 unambiguously demonstrate that the dispersion along the zigzag-chains is much steeper than perpendicular to them. The magnetic structure has to be considered as a weak antiferromagnetic coupling of strongly coupled ferromagnetic zigzag-chains. The obtained magnon dispersion is presented in Fig. 1. The branch propagating along the chains, path  $\Gamma$ -C, is much steeper than the branch propagating perpendicular to it, path  $\Gamma$ -B. At the magnetic zone boundaries C and B we find magnon energies of 19 meV and 6.5 meV, respectively. At the point C where  $\mathbf{q}$  is parallel to the chains, the end-point of the acoustic branch coincides with that of the lowest optic branch, whereas there is a large gap between these branches along the path  $\Gamma$ -B. The magnon branch along the [100]-direction, path  $\Gamma$ -A at  $45^\circ$  to the chains, exhibits an intermediate dispersion. Finally, all zone-boundary modes connect when passing along the zone-boundary paths A-B and A-C.

We have performed measurements around the quarter-integer indexed magnetic zone centers as well as around half-integer indexed ones. As explained above, in elastic scans at these  $\mathbf{Q}$ -values one strictly measures the scattering contribution of the  $\text{Mn}^{3+}$ - and that of the  $\text{Mn}^{4+}$ -sites,

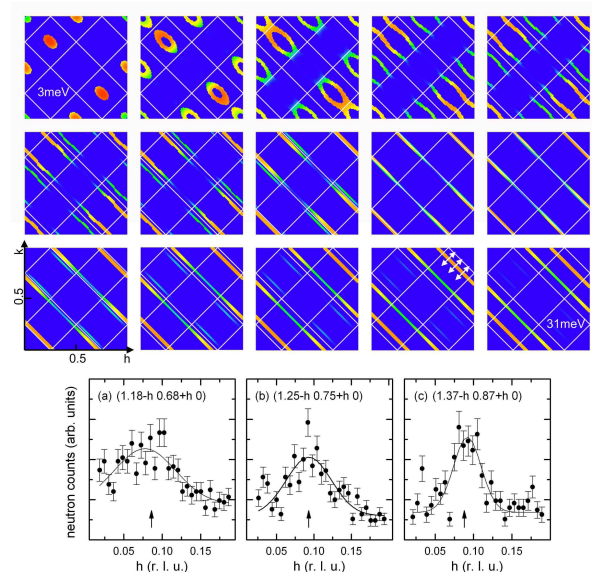


FIG. 3: (color online) Upper panel: Constant energy cuts through the calculated spin-wave structure factor  $S(\mathbf{Q}, \omega)$  with constant energy-resolution of 2 meV within each plot and with energy-steps of 2 meV between adjacent plots, showing the dispersion and scattering distribution of the lowest magnon bands. Lower panel: Constant energy scans along the direction indicated in the 29 meV cut above to experimentally verify the one-dimensional character of the high energy magnetic scattering. The arrows indicate the expected positions of the magnon.

respectively. This separation should hold for inelastic scattering at rather low energies as well. Around these  $\mathbf{Q}$ -values we find exactly the same dispersion, as it is expected for collective magnons. At finite energies there is also a significant structure-factor around the integer-indexed  $\mathbf{Q}$ -values, like (1,0,0); again the dispersion of the modes fully agrees with the other zones. The dispersion shown in Fig. 1 was obtained finally by combining many scans in different magnetic zones. At energies significantly above the saturation of the acoustic magnon branch perpendicular to the zigzag-chains, i.e. 6.5 meV, the magnetic interaction perpendicular to the chains does not play any role anymore and the magnon dispersion exhibits an one-dimensional character.

The spin-wave dispersion has been calculated using the Holstein-Primakoff transformation with a simple spin-only hamiltonian illustrated in Fig. 1a) (in the sums each pair appears only once):

$$\begin{aligned} \mathcal{H} = & - \sum_{(Mn^{3+}, Mn^{4+})_{\parallel}} J_{FM} \mathbf{S}_i \cdot \mathbf{S}_j \\ & + \sum_{(Mn^{3+}, Mn^{4+})_{\perp}} J_{AFM} \mathbf{S}_i \cdot \mathbf{S}_j \\ & - \sum_{(Mn^{3+}, Mn^{3+})_{nnn\parallel}} J_{FM,2} \mathbf{S}_i \cdot \mathbf{S}_j - \sum_{Mn} \Lambda S_z^2. \end{aligned}$$

Details of the calculation can be found in the related

work on the spin excitations in the stripe phases [27]. The  $\text{Mn}^{3+}$  and  $\text{Mn}^{4+}$ -spins were fixed to the values of  $S=2$  and  $S=1.5$ , respectively. Taking into account only the two nearest-neighbor interactions for  $\text{Mn}^{3+}$ - $\text{Mn}^{4+}$ -spin interactions for pairs within and in-between the zigzag-chains,  $J_{FM}$  and  $J_{AFM}$ , one obtains a good description of the measured dispersion denoted in the Fig. 1c) by broken lines. However, there remain significant discrepancies; it is impossible to simultaneously describe the large initial slope of the spin-wave dispersion along the chains and the relatively lower zone-boundary frequencies. This behavior implies the relevance of an additional longer-distance interaction parameter acting along the ferromagnetic chains. Indeed, a fully satisfactory description is obtained by including a ferromagnetic interaction for  $\text{Mn}^{4+}$ - $\text{Mn}^{4+}$ -spin pairs connected through a  $\text{Mn}^{3+}$  within a zigzag-chain [28], see full lines in Fig. 1b). We determine the parameters :  $J_{FM}=9.98\text{ meV}$ ,  $J_{AFM}=1.83\text{ meV}$ ,  $J_{FM,2}=3.69\text{ meV}$  and an anisotropy term of  $\Lambda=0.05\text{ meV}$ . This model predicts the existence of rather flat optical branches around  $75\text{ meV}$  which, however, could not be observed so far due to the high phonon signal at these energies. In contrast with the excellent magnon-dispersion modeling presented above, we do not find a straightforward description of the observed dispersion within the Zener-polaron model. The stacking of magnetic dimers can explain the observed magnetic Bragg-peaks [29], but one would expect the anisotropy of the dispersion around for example  $(0.75, -0.75, 0)$  to be opposite to the experimental finding. This failure and the excellent spin-wave description obtained within the CE-type model give strong support for the latter in  $\text{La}_{1/2}\text{Sr}_{3/2}\text{MnO}_4$ .

Fig. 3 presents the calculated magnon scattering intensities in the form of constant energy cuts. One can see how the anisotropic spin-wave cones develop around the magnetic Bragg-peaks with finite structure factor. At intermediate energies also those magnetic Brillouin-zones contribute where there is no elastic scattering. The Fig. 3 further illustrates that well above the maximum of the acoustic magnon perpendicular to the zigzag-chains, the system looks like a magnetically one-dimensional system. This character was verified by special constant-energy scans, see Fig. 3. The dominant ferromagnetic coupling is furthermore seen in experiments upon heating across the charge and orbital ordering transition. The diffuse magnetic scattering as well as the magnetic fluctuations turn ferromagnetic in character at high temperatures [26].

The ferromagnetic interaction in the COS-phase of  $\text{La}_{1/2}\text{Sr}_{3/2}\text{MnO}_4$  which dominates the spin-wave dispersion is remarkably large. For example it is about a factor of five larger than the ferromagnetic coupling in  $\text{LaMnO}_3$  [30] acting on two  $\text{Mn}^{3+}$ -sites with an antiferroorbital coupling.  $J_{FM}$  is also significantly larger than the ferromagnetic interaction in the metallic ferromagnetic phases with the highest Curie temperatures [12, 13]. In the

Zener double-exchange model a delocalized  $e_g$ -electron mediates the ferromagnetic interaction with the neighbors along three orthogonal directions, whereas the orbitally ordered  $e_g$ -electron in the CE-type phase focuses the magnetic interaction along one direction. The relevance of the additional ferromagnetic coupling reminds the same observation in the metallic phases [15] and implies a similar orbital origin. The dominance of the ferromagnetic interaction in the CE-type phase, which is mediated through the  $e_g$ -orbital, appears to be essential for the capability of manganites to switch between the metallic ferromagnetic and the COS-phases.

In conclusion we have determined the low-energy spin-wave dispersion in the ordered phase of  $\text{La}_{1/2}\text{Sr}_{3/2}\text{MnO}_4$ , which can be excellently described basing on the CE-type structural model of charge, orbital and spin ordering.

Work at Universität zu Köln was supported by the Deutsche Forschungsgemeinschaft through the Sonderforschungsbereich 608. We thank L.P. Regnault for stimulating discussions.

---

\* Electronic address: braden@ph2.uni-koeln.de

- [1] Y. Tokura and N. Nagaosa, *Science* **288**, 462 (2000).
- [2] Y. Momotome et al., *Phys. Rev. Lett.* **91**, 167204 (2003).
- [3] C.P. Adams et al., *Phys. Rev. Lett.* **85**, 3954 (2000).
- [4] S. Shiomura et al., *Phys. Rev. Lett.* **83**, 4389 (1999).
- [5] F.M. Woodward et al., *Phys. Rev. B* **70**, 17443 (2004).
- [6] E.O.Wollan and W.C. Koehler, *Phys. Rev.* **100**, 545 (1955).
- [7] J.B. Goodenough, *Phys. Rev.* **100**, 564 (1955).
- [8] P.G. Radaelli et al., *Phys. Rev. B* **55**, 3015 (1997).
- [9] Z. Jirak et al., *J. Magn. Mat.* **53**, 153 (1985).
- [10] A. Daoud-Aladine et al., *Phys. Rev. Lett.* **89**, 097205 (2002).
- [11] S. Grenier et al., *Phys. Rev. B* **69**, 134419 (2004).
- [12] T. G. Perring et al., *Phys. Rev. Lett.* **77**, 711 (1996).
- [13] H.Y. Hwang et al., *Phys. Rev. Lett.* **80**, 1316 (1998).
- [14] J. W. Lynn et al., *Phys. Rev. Lett.* **76**, 4046 (1996).
- [15] Y. Endoh et al., *Phys. Rev. Lett.* **94**, 017206 (2005).
- [16] Y. Moritomo et al., *Phys. Rev. B* **51**, 3297 (1995).
- [17] S. Larochelle et al., *Phys. Rev. B* **71**, 024435 (2005).
- [18] D. Senff et al., *Phys. Rev. B* **71**, 024425 (2005).
- [19] B.J. Sternlieb et al., *Phys. Rev. Lett.* **76**, 2169 (1996).
- [20] P. Mahadevan et al., *Phys. Rev. Lett.* **87**, 066404 (2001).
- [21] S. Larochelle et al., *Phys. Rev. Lett.* **87**, 095502 (2001).
- [22] S.B. Wilkins et al., *Phys. Rev. Lett.* **91**, 167205 (2003).
- [23] S.S. Dhesi et al., *Phys. Rev. Lett.* **92**, 056403 (2004).
- [24] M. Tokunaga et al., *Phys. Rev. B* **59**, 11151 (1999).
- [25] P. Reutler et al., *J. Cryst. Growth* **249**, 222 (2003).
- [26] D. Senff et al., unpublished data.
- [27] F. Krüger and S. Scheidl, *Phys. Rev. B* **67**, 134512 (2003).
- [28] The magnon dispersion can be described nearly as well when considering a ferromagnetic coupling between two  $\text{Mn}^{3+}$ -sites along the zigzag-chain.
- [29] D.V. Efremov et al., *nature mat.* **3**, 853 (2004).
- [30] F. Moussa et al., *Phys. Rev. B* **54**, 15149 (1996).